Nickel Complexes of 21-Oxaporphyrin and 21,23-Dioxaporphyrin

Piotr J. Chmielewski, Lechosław Latos-Grażyński,* Marilyn M. Olmstead, and Alan L. Balch

Abstract: The nickel(I) and nickel(II) complexes of 5,20-bis(*p*-tolyl)-10,15-diphenyl-21-oxaporphyrin (ODTDPPH) and 5,10,15,20-tetraphenyl-21,23-dioxaporphyrin (O_2TPP) have been investigated. These oxa analogues of 5,10,15,20-tetraarylporphyrin, where one or two pyrrole rings are replaced by a furan moiety, have been synthesized by condensation of the respective precursors, namely 2,5-bis(arylhydroxymethyl)furan, pyrrole, and arylaldehyde. Insertion of nickel(II) into ODTDPPH or O_2TPP yielded high-spin five- and six-coordinate ([(ODTDPP)$\mathrm{Ni^{II}Cl}$] and [(O_2TPP)$\mathrm{Ni^{II}Cl_2}$]) complexes, which can be reduced with moderate reducing reagents. The EPR spectra of [(ODTDPP)$\mathrm{Ni^{I}}$] and [(O_2TPP)$\mathrm{Ni^{I}Cl}$] revealed the $\mathrm{Ni^{I}}$ oxa(dioxa)porphyrin rather than a $\mathrm{Ni^{II}}$ anion radical electronic structure. In the structures of [(ODTDPP)$\mathrm{Ni^{II}Cl}$], [(O_2TPP)$\mathrm{Ni^{II}Cl_2}$], and [(ODTDPP)$\mathrm{Ni^{I}}$], determined by X-ray diffraction, the furan ring is planar and coordinates in the η^1 fashion through the trigonal oxygen atom; the nickel ion lies in the furan plane for the latter two complexes, but slightly outside it in [(ODTDPP)$\mathrm{Ni^{II}Cl}$]. The Ni–N and Ni–O bond lengths decrease upon reduction of high-spin five-coordinate [(ODTDPP)$\mathrm{Ni^{II}Cl}$] to four-coordinate [(ODTDPP)$\mathrm{Ni^{I}}$]. The pattern of downfield pyrrole resonances in ^{1}H NMR spectra of [(ODTDPP)$\mathrm{Ni^{II}Cl}$] and [(O_2TPP)$\mathrm{Ni^{II}Cl_2}$] has been established. The downfield positions of furan resonances are unusual for $\mathrm{Ni^{II}}$ heteroporphyrins; they have been accounted for by the nearly in-plane coordination of the furan moiety as opposed to the side-on coordination found for thiophene- or selenophene-containing heteroporphyrins. An example of ion-pair formation, [$(O_2TPPH)_2$][$\mathrm{Ni^{II}Cl_4}$], was produced from [(O_2TPP)$\mathrm{Ni^{II}Cl_2}$] by acidification with HCl.

Keywords
heterocycles · heteroporphyrins · nickel · porphyrinoids

Introduction

Core modification of porphyrins by the introduction of various heteroatoms (O, S, Se, Te, CH) in place of the nitrogen atoms permits the preparation of a series of new heterocycles that may have interesting properties in terms of both their aromatic character and their ability to bind metal ions. The series of oxygen-containing porphyrins constitutes a group in which the extent of substitution can be systematically varied (Scheme 1).

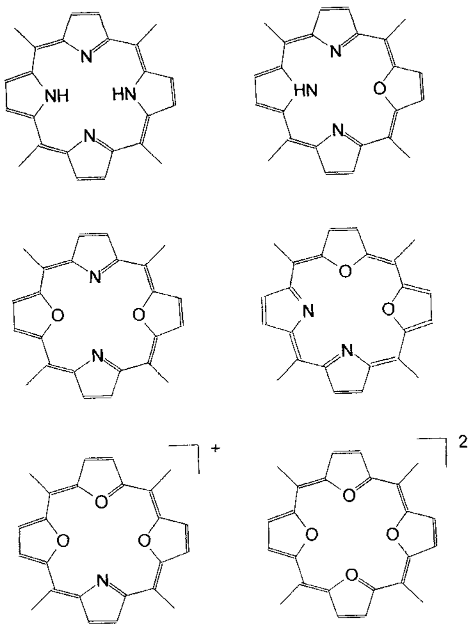

Scheme 1. A series of oxygen-containing porphyrins.

Limited data regarding oxaporphyrins are available. Broadhurst et al. described the synthesis of 8,12,17-triethyl-7,13,18-trimethyl-21-oxaporphyrin, 13,17-diethyl-12,18-dimethyl-21,22-dioxaporphyrin, and 8,17-diethyl-7,18-dimethyl-21,23-dioxaporphyrin.[1, 2] They demonstrated by means of electronic spectroscopy that β-alkylated monooxaporphyrin acts as a tetradentate macrocyclic ligand toward $\mathrm{Zn^{II}}$, $\mathrm{Ni^{II}}$, $\mathrm{Cu^{II}}$, $\mathrm{Co^{II}}$, or $\mathrm{Mn^{II}}$ ions. The zinc(II) and nickel(II) complexes were isolated and characterized by elemental analysis, mass spectra and electronic spectroscopy. However, the β-alkylated dioxaporphyrin failed to form metal complexes by the insertion procedures typ-

---

[*] L. Latos-Grażyński, P. J. Chmielewski
Department of Chemistry, University of Wrocław
50383 Wrocław (Poland)
Fax: Int. code +(71)222-348
e-mail: llg@ichuwr.chem.uni.wroc.pl
M. M. Olmstead, A. L. Balch
Department of Chemistry, University of California, Davis
Davis, California 95616 (USA)

ical for regular porphyrins. The electronic and molecular structures of metalloxaporphyrins have not been studied.

In the search for modifications of oxophlorins (keto tautomers of mesohydroxyporphyrin), 21,22-dioxa-5-oxophlorin and 23,24-dioxa-5-oxophlorin were synthesized.[3] The trioxaporphyrin cation was apparently not prepared. The tetraoxa[18]porphyrin(1.1.1.1) dication was synthesized and discussed in the context of the aromatic character of annulenes.[4] This molecule preserves the general porphyrin framework. In addition, an isomer of porphyrin–porphycene (porphyrin-(2.0.2.0)) possesses its own tetraoxa counterpart, tetraoxaporphyrin(2.0.2.0) dication (tetraoxaporphycene).[4c] The next higher homologues to the tetraoxaporphyrin dication, tetraoxa[22]porphyrin(2.2.2.2) dication and tetraoxa[26]porphyrin-(3.3.3.3) dication, were also obtained.[5]

A general interest in the aromacity of large molecules also prompted investigations of other polyfuran macrocycles, namely, annulenes and annulenones, which were treated as related to expanded porphyrins, although generally these compounds are not aromatic.[6] On the other hand, oxa derivatives of expanded porphyrins exhibit aromaticity. The following expanded porphyrin derivatives with one or two pyrrolic fragments replaced by furan were investigated: dioxasapphyrin,[7] dioxasmaragdyrin,[8] ozaphyrin (isomeric analogue of oxasapphyrin),[7] oxobronzaphyrin (isomeric analogue of rubyrin), and hexaphyrin.[9] To complete the list of oxapolypyrrolic macrocycles one has to include 21,24-dioxacorrole, where two adjacent pyrrole rings were substituted by furans and monoxaporphyrin with an inverted pyrrole ring.[10]

Abstract in Polish: *Zbadano kompleksy niklu(I) i niklu(II) 5,20-bis(p-tolylo)-10,15-difenylo-21-oksaporphyriny (ODTDPPH) i 5,10,15,20-tetrafenylo-21,23-dioksaporphyriny (O_2TPP). Oksa analogi 5,10,15,20-tetrafenyloporfiryny, w których jeden lub dwa pierścienie pirolowe zostały zastąpione przez grupy furanowe tworzą się na drodze kondensacji odpowiedniego prekursora, tj. 2,5-bis(arylohydroksymetylo)furanu, pirolu i aldehydu arylowego. Insercja niklu(II) do ODTDPPH czy O_2TPP daje wysokospinowe kompleksy: pięciokoordynacyjny [(ODTDPP)Ni^{II}Cl] i sześciokoordynacyjny [(O_2TPP)Ni^{II}Cl_2]. Redukcja obu kompleksów została dokonana przy zastosowaniu łagodnych środków redukujących. Widma EPR [(ODTDPP)Ni^{I}] oraz [(O_2TPP)-Ni^{I}Cl] wykazują w obu przypadkach strukturę elektronową kompleksu niklu(I), a nie rodnika anionowego niklu(II).*

Struktury molekularne [(ODTDPP)Ni^{II}Cl], [(O_2TPP)-Ni^{II}Cl_2] i [(ODTDPP)Ni^{I}] zostały wyznaczone rentgenostrukturalnie. We wszystkich strukturach pierścień furanowy jest płaski i koordynuje η^1 przez atom tlenu przyjmujący geometrię trygonalną. Jon niklu leży w płaszczyźnie furanu w przypadku [(ODTDPP)Ni^{I}] i [(O_2TPP)Ni^{II}Cl_2], natomiast w [(ODTDPP)Ni^{II}Cl] obserwuje się nieznaczne jego wychylenie od tej płaszczyzny. Długości wiązań Ni–N i Ni–O są krótsze w czterokoordynacyjnym [(ODTDPP)Ni^{I}] niż w wysokospinowym, pięciokoordynacyjnym [(ODTDPP)Ni^{II}Cl]. Zaobserwowano charakterystyczny wzorzec dolonopolowych przesunięć dla rezonansów protonów pirolowych w widmach ^{1}H NMR [(ODTDPP)Ni^{II}Cl] i [(O_2TPP)Ni^{II}Cl_2]. Niskopolowa lokalizacja sygnału protonów furanowych jest czymś niespotykanym dla serii heteroporfiryn niklu(II). Kierunek przesunięcia kontaktowego furanu związany jest z niemal płaską koordynacją fragmentu furanowego, odmienną od bocznej koordynacji stwierdzonej w porfirynach zawierających tiofen i selenofen.

Zidentyfikowano i scharakteryzowano rentgenostrukturalnie parę jonową [(O_2TPPH)$_2$][Ni^{II}Cl_4] tworzącą się podczas zakwaszania [(O_2TPP)Ni^{II}Cl_2] kwasem solnym.

A complementary area of porphyrin modifications that can be formally described as a replacement of a single atom in the porphyrin skeleton by oxygen concerns 5-oxaporphyrin. Such a molecule is formed during the coupled oxidation of iron porphyrins, which produces verdoheme (iron(III) 5-oxaporphyrin).[11]

Recently our laboratories reported a reasonable synthesis and the structural characterization of a new macrocyclic ligand, 5,20-bis(*p*-tolyl)-10,15-diphenyl-21-oxaporphyrin (ODTDPPH), in which one of the pyrrole groups of 5,10,15,20-tetraarylporphyrin is replaced by furan.[12] In the light of the interesting chemistry of nickel 21-thiaporphyrins[13–15] and nickel 21-selenaporphyrins,[15] we decided to investigate nickel complexes of a 5,10,15,20-tetraaryl-21-oxaporphyrin and 5,10,15,20-tetraaryl-21,23-dioxaporphyrin. We attempted to elucidate the influence of one or two oxygen incorporations in comparison with regular porphyrins and heteroporphyrins. The furan ring, which is regarded as a weak ligand, is a significant component of the oxaporphyrin. There are only a limited number of crystallographically characterized models for furan–metal binding.[17–21] For Sr^{II}, Ba^{II}, Bi^{III}, and Ti^{IV} complexes[16–19] with a furan built into macrocyclic or chelating ligands, coordination occurs through oxygen. Coordination by a carbon atom of furan was observed in lithium tris(α-furyl)$_3$stannate [Sn^{II}-(α-furyl)$_3$Li(α-furyl)$_3$Sn^{II}]$^-$ and in series of low-valent tungsten, rhodium, and iridium complexes.[21]

Here we report on the structure and spectroscopic properties of nickel 21-oxaporphyrin and 21,23-dioxaporphyrin complexes and comment on the relation between coordination geometry and isotropic shifts of the modified ring in a series of nickel(II) heteroporphyrins [(21-X-TPP)Ni^{II}Cl] (X = O, S, Se).

Results

Synthesis: A key step in the synthesis of 5,10,15,20-tetraaryl-21-oxaporphyrin and 5,10,15,20-tetraaryl-21,23-dioxaporphyrin is the construction of the condensation precursor, 2,5-bis(arylhydroxymethyl)furan. Dialcohol substrates for synthesis of thia-, selena-, or telluraporphyrin (STPPH, SeTPPH, TeTPPH), namely 2,5-bis(phenylhydroxymethyl)thiophene, 2,5-bis-(phenylhydroxymethyl)selenophene, or 2,5-bis(phenylhydroxymethyl)tellurophene, were obtained from 1,6-diphenylhexa-2,4-diyne-1,6-diol by a ring closure with H_2S, NaHSe, or NaHTe.[22] Alternatively the preparation of the thiaporphyrin precursor could be achieved by the reaction of the respective 2,5-dilithium derivative with benzaldehyde.[23] To functionalize furan we considered a different approach, which is presented in Scheme 2. This approach uses the reaction of a Grignard reagent with furan-2,5-dicarboxaldehyde. In the adjusted reaction conditions, the asymmetric derivative 2-(phenylhydroxy-

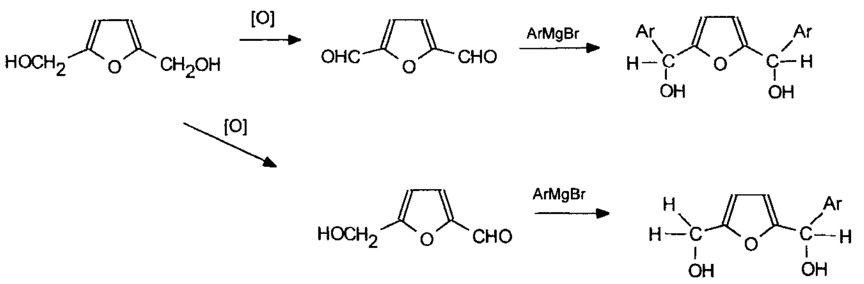

Scheme 2. Furan functionalization by means of the reaction of a Grignard reagent with furan-2,5-dicarboxaldehyde.

methyl)-5-(hydroxymethyl)furan is formed along with 2,5-di(phenylhydroxymethyl)furan.

21-Oxatetraphenylporphyrin can be prepared in reasonable yield from 2,5-di(phenylhydroxymethyl)furan by a procedure analogous to that described previously for 21-thiaporphyrin[15a] or 21-selenaporphyrin.[16] The synthetic route to 21-oxatetraarylporphyrin is shown in Scheme 3. The synthesis involves a

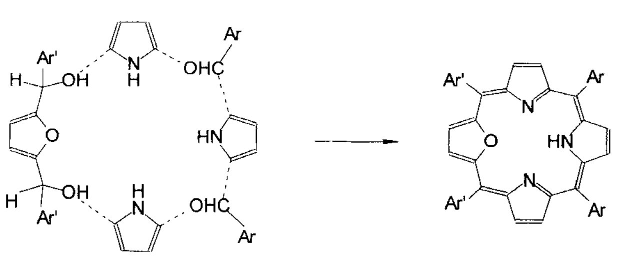

Scheme 3. Synthetic route to 21-oxatetraarylporphyrin.

one-pot reaction from 2,5-bis(p-tolylhydroxymethyl)furan, benzaldehyde, and pyrrole in dichloromethane, as described briefly in our communication.[12] The procedure can introduce unsymmetrical substituents on the porphyrin periphery in a structurally defined relationship to the location of the furan ring. With 2-(phenylhydroxymethyl)-5-(hydroxymethyl)furan and p-tolylaldehyde present in the reaction mixture we obtained 10,15-bis(p-tolyl)-20-phenyl-21-oxaporphyrin (OPDTPH).

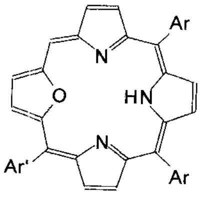

OPDTPH

The synthetic work on 5,10,15,20-tetraphenyl-21,23-dioxaporphyrin (O_2TPP) is sum-marized in Scheme 4. The dioxaporphyrin was synthesized by the condensation of pyrrole and 2,5-bis(phenylhydroxymethyl)furan under similar conditions to those used for the preparation of monooxaporphyrins.

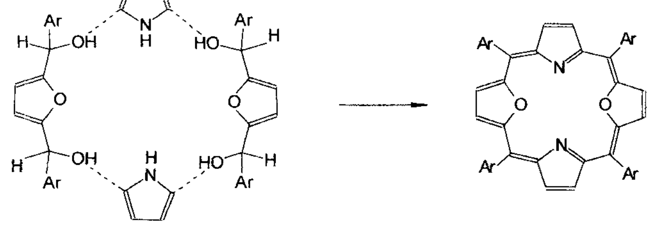

Scheme 4. Synthesis of O_2TPP.

The electronic spectra of ODTDPPH and O_2TPP are shown in Figure 1. The spectra resemble the electronic spectra of $TPPH_2$ and its other tetraarylheteroanalogues.[12,16,22–24] A distinction has been made between the intense Soret band in the near ultraviolet and four Q bands in the visible region. Relative to $TPPH_2$ a strong bathochromic shift of the QI band of ODTDPPH is observed. In O_2TPP the introduction of the two oxygen atoms causes a strong bathochromic shift of the QI and QII bands and a hypsochromic shift of QIII and QIV compared with $TPPH_2$. In the series oxa-, thia-, selena-, and telluraporphyrin systematic bathochromic shifts have been found for the Soret and all Q bands. However, in the series O_2TPP, S_2TPP, Se_2TPP, the marked bathochromic shifts are determined only for the Soret and QIV and QIII bands. The dioxaporphyrin shows the QI band with the lowest energy (λ_{max} = 704 nm) of all heteroporphyrin systems investigated until now.

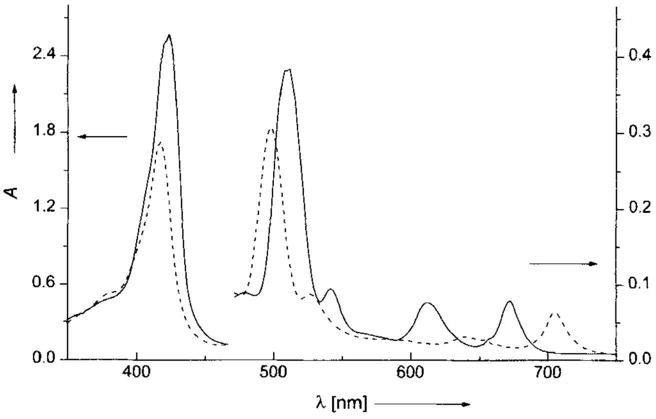

Figure 1. UV/Vis spectra of oxaporphyrins (dichloromethane, 293 K). Solid line = ODTDPPH, dashed line = O_2TPP.

The spectroscopic properties of ODTDPPH and O_2TPP suggest that they have aromatic character; this is consistent with the presence of $4n + 2\,\pi$ electrons. The aromaticity of oxaporphyrin and dioxaporphyrin is confirmed by the ^1H NMR shifts of the pyrrole protons (ODTDPPH: $\delta = 8.82$ *trans*, 8.62, 8.57 *cis*; O_2TPP: $\delta = 8.38$) and furan resonances (ODTDPPH: $\delta = 9.21$, O_2TPP: $\delta = 9.10$), and the upfield position of the NH resonance of ODTDPPH ($\delta = -1.58$). These values are accounted for by the ring-current effect, which is specific for aromatic macrocyclic systems.

Formation and characterization of nickel(II) complexes: Insertion of nickel(II) into 5,10,15,20-tetraphenyl-21-oxaporphyrin was readily achieved under moderate conditions by boiling a mixture of ODTDPPH in chloroform and an ethanolic solution of nickel(II) chloride hydrate. When applied to 5,10,15,20-tetraphenyl-21,23-dioxaporphyrin, the procedure yielded a six-coordinate $[(O_2TPP)Ni^{II}Cl_2]$ complex. The electronic absorption spectra of $[(ODTDPP)Ni^{II}Cl]$ and $[(O_2TPP)Ni^{II}Cl_2]$ are shown in Figure 2. A porphyrin-like spectrum is clearly present for [(ODTDPP)Ni^{II}Cl] with a Soret band and the three Q bands. The electronic spectrum of [(O_2TPP)Ni$^{II}Cl_2$] is similar to the spectrum of O_2TPP (Figure 1). The coordination causes only minor shifts in the band positions. The spectral similarities suggest that the nickel(II) insertion does not influence the geometry of the dioxaporphyrin chromophore.

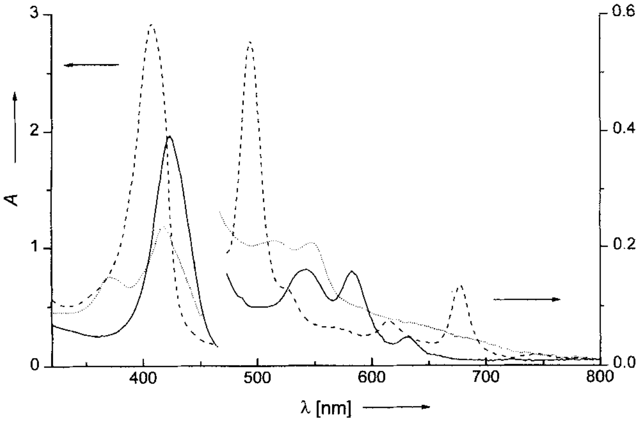

Figure 2. UV/Vis spectra of nickel oxaporphyrin complexes. Solid line = [(ODTDPP)Ni^{II}Cl] (dichloromethane), dashed line = [(O_2TPP)Ni$^{II}Cl_2$] (dichloromethane), dotted line = [(ODTDPP)Ni^{I}] (benzene).

The acidic demetalation of [(ODTDPP)Ni^{II}Cl] and [(O_2TPP)-Ni$^{II}Cl_2$] in a dichloromethane/hydrochloric acid mixture gave ODTDPPH and O_2TPP, respectively, after chromatographic work-up. However, the evaporation of the dichloromethane layer produced in the course of [(O_2TPP)Ni$^{II}Cl_2$] demetallation yields the unusual nickel(II)–dioxaporphyrin compound formulated as (O_2TPPH)$_2$[Ni$^{II}Cl_4$], where two monoprotonated dioxaporphyrins act as monocations neutralizing a $[NiCl_4]^{2-}$ anion. The electronic spectrum of (O_2TPPH)$_2$[Ni$^{II}Cl_4$] (not shown) is similar to O_2TPP with slightly broadened bands. The [(ODTDPP)Ni^{II}Cl] and [(O_2TPP)Ni$^{II}Cl_2$] complexes are paramagnetic ($S = 1$), demonstrated by the distinctive isotropic shift of pyrrole and phenyl resonances (Figure 3) in their ^{1}H NMR spectra. However, the ^{1}H NMR spectrum of (O_2TPPH)$_2$-[Ni$^{II}Cl_4$] bears the features of a diamagnetic species. The (O_2TPPH)$^+$–[Ni$^{II}Cl_4$]$^{2-}$ ion pair seems to be not tightly bound in the chloroform solution.

NMR studies of paramagnetic nickel(II) complexes: The ^{1}H NMR spectra of the paramagnetic [(ODTDPP)Ni^{II}Cl], [(OPDTP)-Ni^{II}Cl] and [(O_2TPP)Ni$^{II}Cl_2$] are shown in Figures 3 and 4. The spectral parameters for these and other relevant compounds have been gathered in Table 1. The spectroscopic data for [(ODTDPP)Ni^{II}Cl], [(OPDTP)Ni^{II}Cl], and [(O_2TPP)Ni$^{II}Cl_2$] have been analyzed by consideration of their effective symmetry in solution. [(ODTDPP)Ni^{II}Cl] appears to have effective C_s geometry with the mirror plane passing through the nickel atom, the chloride, and the furan oxygen. In this case there are three distinct pyrrole protons and one furan proton. Two *ortho* and two *meta* positions on each phenyl ring will be distinguishable by ^{1}H NMR unless the rotation around the $C_{meso}-C_{\alpha}$ bond is sufficiently fast.[25] The ^{1}H NMR spectrum of [(OPDTP)-Ni^{II}Cl] has been analyzed in the light of its C_1 symmetry. There

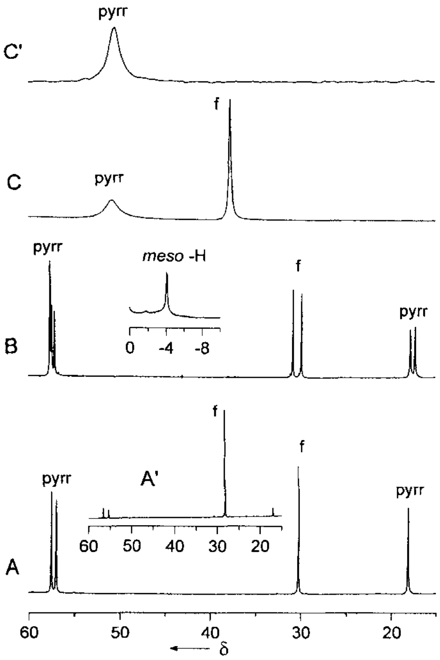

Figure 3. NMR spectra (293 K) of: A) [(ODTDPP)Ni^{II}Cl] (CDCl$_3$, ^{1}H NMR); A′) ([D_6]ODTDPP)Ni^{II}Cl] (C_7D_8, ^{1}H NMR); B) [(OPDTP)Ni^{II}Cl]; C) [(O_2-TPP)Ni$^{II}Cl_2$] (CDCl$_3$, ^{1}H NMR); C′) [([D_4]O_2TPP)Ni$^{II}Cl_2$] (CHCl$_3$, ^{2}H NMR). Peak labels: pyrr: pyrrole ring protons; *meso*: 5-CH; f: furan.

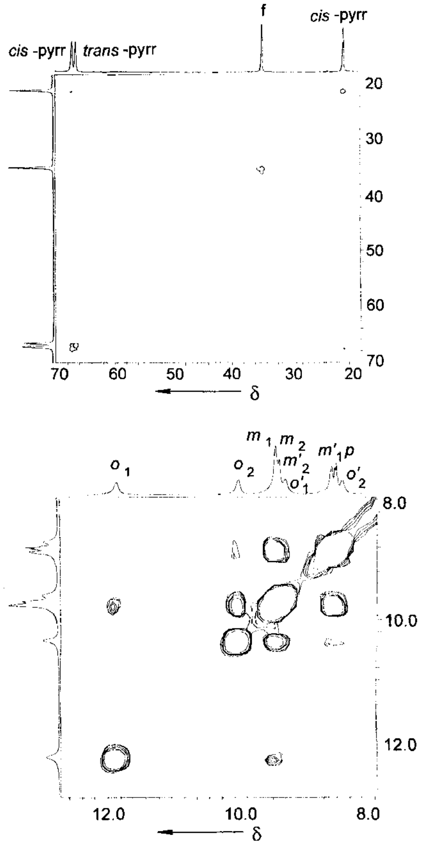

Figure 4. The 2D ^{1}H COSY spectrum of [(ODTDPP)Ni^{II}Cl] (CDCl$_3$, 273 K). Upper map: lowfield region showing spin–spin coupling of regular pyrrole protons; lower map: *meso*-phenyl region. Peak labels: *trans*-pyrr and *cis*-pyrr denote 7,8,17,18- and 12,13- pyrrole protons, respectively; f: furan; *o*, *m*, *p* denote resonances of *ortho*, *meta*, or *para* protons of 10,15-phenyl rings; *o*′, *m*′ are assigned to *ortho* and *meta* protons of 5,20-*p*-tolyl groups.

Table 1. ^{1}H NMR data for nickel(II) heteroporphyrins [a].

	cis-Pyrrole	*trans*-Pyrrole	Modified heterocycle	*meso*-Aryls
$[(ODTDPP)Ni^{II}Cl]$	57.53, 18.12	56.92	30.23	11.43, 9.80, 9.24, 9.17, 9.07, 8.47, 8.46, 8.43, 3.82 (*p*-CH_3)
$[(OPDTP)Ni^{II}Cl]$	57.40, 57.60, 17.77, 17.23	57.60, 57.08	30.72, 29.79	11.73, 11.03, 9.72, 9.31, 9.22, 9.15, 8.93, 8.61, 8.27, 8.12, 7.91, 3.55, 3.49 (*p*-CH_3), −4.08 (*meso* H)
$[(O_2TPP)Ni^{II}Cl_2]$	50.86		37.72	8.97, 8.24, 8.15
$[(STPP)Ni^{II}Cl]$[b]	64.58, 32.52	30.91	−29.84	9.93, 9.81, 9.74, 8.10, 7.31, 6.53, 6.17
$[(SeDPDTP)Ni^{II}Cl]$[c]	68.32, 40.21	17.09	−38.75	10.76, 10.23, 9.75, 9.44, 8.66, 6.94, 6.30, 5.72

[a] All spectra recorded in $CDCl_3$ solution at 295 K. [b] Ref. [13b]. [c] Ref. [16].

are six distinct pyrrole positions, two furan positions, three nonequivalent *meso* phenyl rings, and one *meso* proton. In the NMR spectrum the lowered symmetry in comparison with $[(ODTDPP)Ni^{II}Cl]$ is reflected by the doubling of each pyrrole and furan resonance. A higher effective symmetry, D_{2h}, can be predicted for $[(O_2TPP)Ni^{II}Cl_2]$. Such a geometry generates only one pyrrole resonance and one furan resonance. The *meso* phenyl rings are symmetrically equivalent, and produce only three resonances. Their *ortho* and *meta* positions are pairwise equivalent because of the mirror symmetry with respect to the porphyrin plane. As well as geometrical considerations, relative intensities, line widths, site-specific deuteration, and 2D COSY experiments were used as the basis for the resonance assignments, which are given above each peak in Figure 3. The most characteristic feature for $[(ODTDPP)Ni^{II}Cl]$, the downfield resonance at $\delta = 30.2$, has been assigned to the furan β-protons. In order to distinguish the pyrrole and furan resonances, the ^{1}H NMR spectrum of $[([D_6]ODTDPP)Ni^{II}Cl]$ was recorded, and is shown as trace A′ in Figure 3. The three pyrrole resonances are in the $\delta = 60-20$ region. The additional resonances, presented in detail in Figure 4, come from the *meso* phenyl protons. In the case of $[(O_2TPP)Ni^{II}Cl_2]$ the furan resonance has been unambiguously identified at $\delta = 37.7$, since it is absent in the ^{2}H NMR spectrum of $[([D_4]O_2TPP)Ni^{II}Cl]$ where the ligand is deuterated in all β-pyrrole positions. (Figure 3, Table 1).

The two-dimensional COSY experiment is effective in connecting protons within pyrrole moieties and *meso* phenyl groups of metallotetraarylporphyrins.[16, 26–28] Figure 4 shows representative COSY data collected in [D]chloroform solution at 253 K. Crosspeaks reveal pairwise coupling between 7-H and 8-H (17-H and 18-H) pyrrole resonances ($\delta = 57.5$ and 18.1), denoted as *cis*-pyrr in Figure 4. No crosspeak is observed for the resonance assigned to the 12-H, 13-H protons (*trans*-pyrr) by default. Characteristic sets of crosspeaks resulting from coupling between five protons of a phenyl ring have been established and located in the COSY map for the two nonequivalent phenyl rings of $[(ODTDPP)Ni^{II}Cl]$. The two *ortho* and *meta* protons on each of the *meso* phenyl or *meso* tolyl rings are nonequivalent, since the porphyrin plane bears different substituents on the opposite sides and rotation about the *meso* carbon–phenyl bond is restricted.

Analysis of hyperfine shifts: Curie plots of the temperature dependences of the chemical shifts of the $[(ODTDPP)Ni^{II}Cl]$ and $[(O_2TPP)Ni^{II}Cl_2]$ pyrrole and furan resonances (not shown) are linear, with extrapolated intercepts that do not correspond to the appropriate diamagnetic references. Thus there is a small contribution to the dipolar shift from the anisotropy of zero-field splitting (ZFS). The ZFS contribution results in T^{-2}-dependent curvature.[29, 30] However, the alternate directions of the phenyl shifts in $[(ODTDPP)Ni^{II}Cl]$ and $[(O_2TPP)Ni^{II}Cl_2]$ are compatible with the dominant π-contact contribution with a negligible dipolar contribution. This is consistent with the ground state of Ni^{II}, which has two unpaired electrons in the σ-symmetry orbitals $(d_{x^2-y^2})^1(d_{z^2})^1$. The downfield shifts of three pyrrole and furan resonances are indicative of σ-delocalization of spin density.

The unprecedented downfield isotropic shift of the furan ring is important as regards the nature of the interaction in the series of nickel(II) 21-heteroporphyrin complexes including *N*-methylated porphyrins and *C*-methylated inverted porphyrins.[13, 15c, 16, 31] Previously we have always observed an *upfield* isotropic shift of the modified pyrrole ring proton resonances and discussed the π delocalization of the unpaired spin density in nickel(II) heteroporphyrins and nickel(II) *N*-methylporphyrins in terms of ligand-to-metal and metal-to-ligand charge transfer. The strong tilt of the modified ring changes the geometry of the spin density delocalization path as compared with the regular pyrrole rings. The unpaired spin density was localized on the molecular orbital dominated by the p_z component, which can transfer the σ spin density but simultaneously contributes to the π orbitals of the modified ring. The considerable differences in the spin densities at the particular pyrrole carbons were related to the pattern of the occupied π and unoccupied π* molecular orbitals.[13, 16]

In the case of $[(ODTDPP)Ni^{II}Cl]$ and $[(O_2TPP)Ni^{II}Cl_2]$, the downfield position of the furan resonances implies that the coordination geometry of the furan ring is similar to that of the pyrrole rings. Consequently, the downfield contact shift is determined by a σ delocalization mechanism. Such a structure–isotropic shift relation is consistent with our crystallographic studies (vide infra).

Chemical reduction of $[(ODTDPP)Ni^{II}Cl]$ and $[(O_2TPP)Ni^{II}Cl_2]$: Moderate reducing agents are sufficient to carry out one-electron reduction of both $[(ODTDPP)Ni^{II}Cl]$ and $[(O_2TPP)Ni^{II}Cl_2]$.[32] Reduction in benzene by aqueous sodium dithionite or zinc amalgam produced nickel(I) derivatives. To avoid any complication with axial ligation, zinc amalgam has been used for the preparative reduction according to reactions (1) and (2): $[(ODTDPP)Ni^{I}]$ was isolated as a dark solid;

$$[(ODTDPP)Ni^{II}Cl] + e^- \longrightarrow [(ODTDPP)Ni^{I}] + Cl^- \qquad (1)$$

$$[(O_2TPP)Ni^{II}Cl_2] + e^- \longrightarrow [(O_2TPP)Ni^{I}Cl] + Cl^- \qquad (2)$$

Table 2. Selected interatomic distances and bond angles for nickel oxaporphyrins.

	$[(ODTDPP)Ni^{II}Cl]$	$[(O_2TPP)Ni^{II}Cl_2]$	$[(ODTDPP)Ni^{I}]$	$(O_2TPPH)[Ni^{II}Cl_4]$	ODTDPP [a]	furan [b]
Ni–O(1)	2.185(5)	2.133(4)	2.120(3)			
Ni–N(1)	2.004(6)	2.001(4)	1.950(4)			
Ni–N(2)	1.955(5)		1.952(4)			
Ni–N(3)	2.063(5)		2.065(4)			
O(1)–C(1)	1.397(8)	1.373(6)	1.390(5)	1.376(8)	1.380(4)	1.370
C(1)–C(2)	1.429(10)	1.400(8)	1.421(6)	1.402(10)	1.403(4)	1.322
C(2)–C(3)	1.355(10)	1.374(8)	1.355(6)	1.353(10)	1.363(4)	1.425
Ni–Cl	2.293(2)	2.428(2), 2.400(2)		2.254(4), 2.289(4), 2.292(4), 2.285(4)		
O(1)-Ni-N(2)	163.9(2)	179.55(14) [c]	177.7(2)			
N(1)-Ni-N(3)	158.7(2)	179.8(2) [d]	172.4(2)			
C(1)-O(1)-C(4)	107.3(5)	107.8(4)	106.4(3)	107.3(5)	107.0(5)	
O(1)-C(1)-C(2)	107.6(6)	108.5(5)	108.6(4)	108.1(5)	108.0(6)	
C(1)-C(2)-C(3)	108.0(6)	107.7(5)	107.9(4)	108.8(6)	108.0(5)	

[a] Ref. [12]. [b] Ref. [43]. [c] O(1)-Ni-O(2). [d] N(1)-Ni-N(2).

$[(O_2TPP)Ni^{I}Cl]$ was generated directly before any spectroscopic characterization, but not isolated. The electronic spectra of the one-electron reduced species are included in Figure 2. The chemical reductions are reversible. Addition of oxidants (O_2, I_2) regenerates the nickel(II) complexes.

The EPR spectra of the reduction products as frozen toluene solutions at 77 K are shown in Figure 5. Well-defined rhombic patterns are observed with $g_1 = 2.168$, $g_2 = 2.116$, $g_3 = 2.097$ ($g_{iso} = 2.130$ at 293 K) for $[(ODTDPP)Ni^{I}]$ and $g_1 = 2.295$, $g_2 = 2.141$, $g_3 = 2.090$ ($g_{iso} = 2.144$ at 293 K) for $[(O_2TPP)Ni^{I}Cl]$. The electronic structure of one-electron reduced species can be discussed in terms of two canonical forms: nickel(I) oxaporphyrin (dioxaporphyrin) and nickel(II) oxaporphyrin (dioxaporphyrin) anion radicals.[15] Alternatively, the reduced molecules can be considered as metallomacrocyclic radicals with varied metallic contribution to the singly occupied MO. The EPR spectral parameters highlight the strong contribution of the d^9 electronic structure to the ground-state description and corroborate the formulations $[(ODTDPP)Ni^{I}]$ and $[(O_2TPP)Ni^{I}Cl]$.

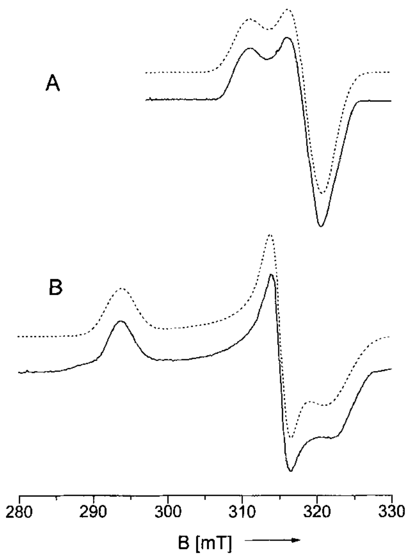

Figure 5. EPR spectra (toluene, 77 K) of: A) $[(ODTDPP)Ni^{I}]$, B) $[(O_2TPP)Ni^{I}Cl]$. The solid line corresponds to experimental spectra. Simulated spectra are shown as dashed lines.

Crystal and molecular structures of $[(ODTDPP)Ni^{I}]$, $[(ODTDPP)Ni^{II}Cl]$, $[(O_2TPP)Ni^{II}Cl_2]$, and $(O_2TPPH)_2[NiCl_4]$: The structures have been studied by X-ray diffraction. The perspective views of the complexes are shown in Figures 6–9. A selection of important bond distances and angles are reported in Table 2. The structure of $[(ODTDPP)Ni^{II}Cl]$ displays disorder in the location of the furan oxygen and one of the *cis* pyrrolic nitrogens. Figure 6 only shows the major form. The nickel is displaced 0.3289 Å out of the O(1)N(1)N(2)N(3) plane toward the axial chloride. The deviation of the pyrrole planes from the plane defined by dihedral angles between the pyrrole (furan) and O(1)N(1)N(2)N(3) planes are as follows: O(1) 9.5°, N(1) −12.9°, N(2) 7.0°, N(3) −8.6°. This can be described as a saddle distortion mode for the oxaporphyrin macrocycle. The Ni–N bond lengths are similar to the 2.038(4) Å seen in a six-coordinate, high-spin nickel(II) porphyrin complex[33] or 2.09 Å in a six-coordinate high-spin nickel(II) hydroporphyrin com-

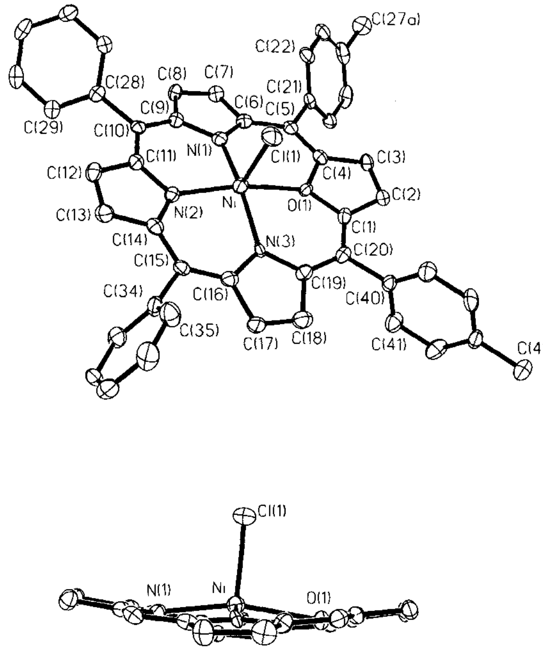

Figure 6. A perspective drawing (with 50% probability ellipsoids) of $[(ODTDPP)Ni^{II}Cl]$ showing the major molecule orientation. The lower view in which aryl groups are omitted emphasizes deviations from planarity.

plex.[34] The similarities of bond lengths to those found for the five-coordinate, high-spin nickel(II) tetraphenyl-21-thiaporphyrin,[13a] 2.094(3), 1.963(3), and 2.084(3) Å, and high-spin five-coordinate nickel(II) *C*-methylated inverted porphyrin,[31b] 2.030(8), 2.057(8), and 1.978 Å, have also been noted. The furan ring is planar and coordinates in the η^1 fashion through an oxygen atom, which acquires trigonal geometry. Thus the nickel(II) lies slightly above the furan plane with the angle between the O(1)C(1)C(2)C(3)C(4) plane and the Ni–O(1) bond being 17.0°. In [(STPP)Ni^{II}Cl] the corresponding angle between the SC(2)C(4) plane and the Ni–S bond is 63.3°.[13a] The Ni^{II}–O distance is longer than the sum of the Pauling covalent radii of octahedral nickel(II) (1.39 Å) and oxygen (0.66 Å) but falls in the broad range observed for nickel(II)–ether oxygen bond distances (1.99–2.31 Å).[35]

The structure of nickel(II) dioxaporphyrin (Figure 7) consists of ordered molecules of [(O$_2$TPP)Ni^{II}Cl$_2$] and disordered molecules of dichloromethane. The Ni–N and Ni–O bond length are, as expected, similar to those of other paramagnetic nickel(II) porphyrin (heteroporphyrin) complexes but slightly shorter than those measured for [(ODTDPP)Ni^{II}Cl]. The dioxaporphyrin skeleton is essentially planar. The furan ring is planar and coordinates in the η^1 fashion through the oxygen atom, which acquires trigonal geometry. Thus the nickel(II) is practically coplanar with the furan ring. The Ni^{II}–Cl(1) (2.428(2) Å) and Ni^{II}–Cl(2) (2.400(2) Å) bonds are the longest found for high-spin nickel(II) heteroporphyrins ([(ODTDPP)Ni^{II}Cl] 2.293(2), [(STPP)Ni^{II}Cl] 2.275(1) Å),[13a] but a comparable Ni–Cl length (2.492 Å) was observed in [Ni^{II}(cyclam)Cl$_2$].[36] This considerable lengthening of the Ni–Cl bonds can be ascribed to the mutual *trans* interaction of axial chloride ligands. A similar phenomenon was previously noted in the [(β-PPh$_3$–TPP)Fe^{III}Cl$_2$] structure in comparison with [(TPP)Fe^{III}Cl].[37]

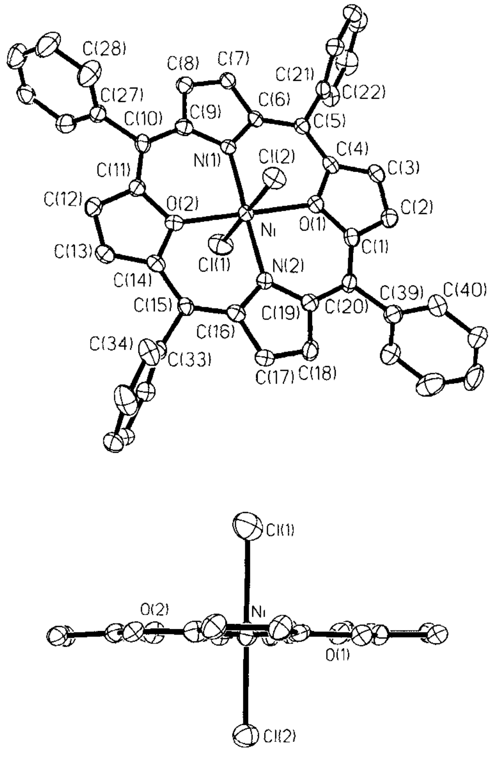

Figure 7. A perspective view (with 50% probability ellipsoids) of [(O$_2$TPP)Ni^{II}Cl]. The lower drawing emphasizes deviations from planarity.

The locations of the oxygen atom and one of the *cis*-nitrogen atoms in the structure of [(ODTDPP)Ni^{I}] are disordered. The other nitrogen atoms are not involved in the disorder. Figure 8 shows only the major form; here also nickel is located in the furan plane and the furan ring coordinates in η^1 fashion through the oxygen atom, which acquires trigonal geometry. In contrast, the relevant angle between the Ni–S bond and the S(2)C(4) plane of [(STPP)Ni] is 45.9°.[15b] The coordination center of the (ODTDPP)Ni^{I} molecule is nearly planar. The nickel is slightly displaced (0.0683 Å) out of the O(1)N(1)N(2)N(3) plane. The deviation of the pyrrole planes from the plane defined by the dihedral angles between the pyrrole and O(1)N(1)N(2)N(3) planes are as follows: O(1) 5.5°, N(1) −14.8°, N(2) 7.2°, N(3) −14.8°. This geometry corresponds to a saddle distortion mode for the oxaporphyrin macrocycle.

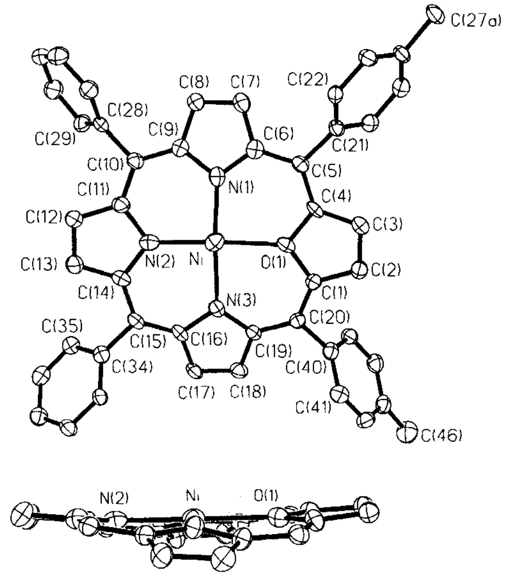

Figure 8. A perspective drawing (with 50% probability ellipsoids) of [(ODTDPP)Ni^{I}], showing the major molecular orientation. The lower view, in which the aryl groups are omitted, emphasizes deviations from planarity.

Examination of the data in Table 2 indicates that the Ni–N and N–O bond lengths decrease upon reduction of the high-spin, five-coordinate [(ODTDPP)Ni^{II}Cl] to four-coordinate [(ODTDPP)Ni^{I}]. These Ni^{I}–N(1) and Ni^{I}–N(2) distances located in the ordered fragment of [(ODTDPP)Ni^{I}] are even shorter than those determined for [(O$_2$TPP)Ni^{II}Cl$_2$]. The Ni^{I} distances of [(ODTDPP)Ni^{I}] are shorter than those of four-coordinate nickel(I) thiaporphyrin.[15b] Ni–O bond lengths of [(ODTDPP)Ni^{II}Cl] and [(ODTDPP)Ni^{I}] follow the trend determined for Ni–N bonds, although the disorder in these fragments renders such a comparison of the limited value. Analogously to the [(STPP)Ni^{II}Cl]–[(STPP)Ni^{I}] couple, this comparison shows that the reduction does not necessarily imply expansion of all metal–ligand distances; for example, the pattern of two shorter and two longer Ni^{I}–N distances was determined in several Ni(I) tetraaza complexes characterized by EXAFS or X-ray diffraction.[38] In the cases where the coordination number is lowered, a lack of expansion upon reduction is fairly general phenomenon.[39] There are also examples in which reduction without ligand loss is accompanied by a decrease in metal–ligand distance.[40] Previously the dramatic shortening of the Ni–S bond that occurred upon reduction of [(STPP)Ni^{II}Cl] was considered to reflect π back-donation, which could be responsible for the stabilization of the one-electron reduction product.[15b] The replacement of the sulfur by oxygen still produces a macrocycle which stabilises low oxidation states of nickel. This observation excludes a special role of the sulfur in the stabilization of nickel(I).

For comparison the structures of some of the free ligands are known. The structure of ODTDPPH was investigated previously.[12] Here we present the structure of [(O$_2$TPPH)$_2$][NiCl$_4$], where the dioxaporphyrin monocation formed by protonation of one of the pyrrole nitrogens has been found. The hydrogen atom of the NH group was clearly located on a difference map and its position was subsequently refined. The cation is puckered, as seen in Figure 9. The nonbonded distances (N(1)–N(2) 4.00, O(1)–O(2) 4.25 Å) compared with the N–N distances in the monoxaporphyrin[12] and in TPPH$_2$ suggest that molecule is *not* elongated.[41] The unit cell also contains five disordered molecules of dichloromethane. The nickel(II) coordination conforms to expectations for a tetrachloronickel(II) anion. The Ni^{II}–Cl distances, 2.254(4), 2.289(4), 2.292(4), and 2.283(4) Å, are comparable to the 2.246–2.272 Å range determined for [NiCl$_4$]$^{2-}$.[42]

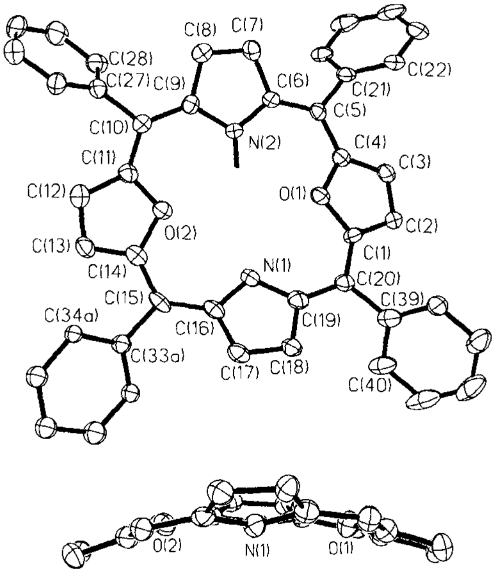

Figure 9. Perspective view of (O$_2$TPPH)$^+$ as found in (O$_2$TPPH)$_2$[NiCl$_4$] with 50% thermal contours for all non-hydrogen atoms. A second view with aryl groups omitted shows deviation from planarity.

In the monooxa-and dioxaporphyrins and their nickel complexes, the O–Cα, C$_\alpha$–C$_\beta$, C$_\beta$–C$_\beta$ bond lengths are practically identical (Table 2). The aromatic character of the macrocycle has an appreciable effect on the furan portions. Thus in these macrocycles the C$_\alpha$–C$_\beta$ distances are longer and the C$_\beta$–C$_\beta$ distances are shorter than in free furan.[43] The pattern of C$_\alpha$–C$_\beta$ and C$_\beta$–C$_\beta$ distances follows that seen in the pyrrole rings. These bond changes indicate that the π delocalization through the furan ring is altered in monoxa- and dioxaporphyrins and their nickel complexes. However, the C$_\alpha$–O bond lengths remain practically unchanged compared with those in furan. These changes suggest that the π electron density has been altered within the furan portion so that it is increased in the C$_\beta$–C$_\beta$ bond, decreased in the C$_\alpha$–C$_\beta$ bond, and unchanged in the C$_\alpha$–O bonds. A similar influence of the aromatic macrocycle on the delocalization pattern in the modified ring was observed in the case of tetraoxa[18]porphyrin(1.1.1.1) dication,[41] ozaphyrin,[8] and thia- and dithiaporphyrin.[44]

Discussion

The porphyrin core is well recognized as providing a stable yet somewhat flexible environment for the coordination of a great variety of metal ions. Introduction of other atoms (O, S, Se, Te, or CH) produces new porphyrin-like macrocycles that are of interest for use as new complexing agents.[1–4, 12–16, 22–24, 45, 46] The incorporation of furan, thiophene, selenophene, or tellurophene rings in place of a pyrrole alters the character of the macrocycle significantly. The presence of the large heteroatoms shrinks the porphyrin core relative to that of regular porphyrin TPPH$_2$: STPPH N···S 3.547(8), N···N 4.40(1) Å;[44] SeTPPH N···Se 3.36, N···N 4.49 Å;[16] TeTPPH N···Te 3.13(1), N···N 4.65(2) Å;[12] S$_2$TPP S···S 3.069(6), N···N 4.65(1) Å;[44] Se$_2$TPP Se···Se 2.91 Å;[22] SSeTPP S···Se 2.89 Å;[22] STeTPP S···Te 2.65 Å;[22] TPPH$_2$ tetragonal N···N 4.108 Å; triclinic 4.06, 4.20 Å.[41] When considering complex formation between a metal and complexing porphyrin or heteroporphyrin, the matching of macrocycle cavity size to metal radius is of prime importance.[47] The heteroporphyrin may be capable of modification by stepwise controlled changes in its cavity size. In oxa and dioxaporphyrins the size of the porphyrin-coordinating center ODTDPPH (N···O 4.132 Å; N···N 4.034 Å) and O$_2$TPPH (O···O 4.25 Å; N···N 4.00 Å) is comparable to that of regular porphyrin, since the atomic radii of nitrogen and oxygen are alike. We are thus able to anticipate a similar match for a large variety of metal ions including nickel(I) and nickel(II) for the radius of the cavity in porphyrin and oxaporphyrins, a situation radically different from that found for thiaporphyrin or selenaporphyrin.

This study has established a number of significant characteristics of the oxa and dioxa core-modified porphyrins. Although furan is generally considered to be a poorly coordinating ligand,[17–21] within the macrocyclic structure provided by these core-modified porphyrins furan can function as a donor toward nickel. In both the oxa and dioxa macrocycles, the furan rings coordinate nickel so that the metal ion resides in the plane of the furan ring and the furan ring is nearly coplanar with the rest of macrocycle. In this sense, the nickel complex of oxaporphyrin contrasts markedly with the nickel complexes of the thiaporphyrin and selenaporphyrin, where the coordinated thiophene and selenophene rings are sharply bent out of the porphyrin plane.[13, 15] As a consequence of the planarity of the oxaporphyrins, the ^{1}H NMR resonances of the furan protons exhibit similar hyperfine shifts to those of the pyrrole protons. In contrast, in the thiaporphyrin and selenaporphyrin nickel complexes, the protons of the thiophene and selenophene ring exhibit opposing hyperfine shifts to those of the pyrrole protons.[13, 15] The oxaporphyrin ligand, just like the thiaporphyrin ligand, is able to stabilize the relatively uncommon Ni(I) oxidation state.[15, 38, 49–51] Thus the sulfur atom of the thiaporphyrin is not in fact responsible for some unusual effect that stabilizes Ni(I).

Interest in the chemistry of Ni(I) complexes is prompted by reactivity studies of F430, a Ni^{II} hydrocorphinoid complex that is the prosthetic group of methyl coenzyme M reductase. EPR data have already pointed to the importance of the Ni(I) in the enzymatic mechanism.[38, 47, 49–51]

Considering their properties, the oxa- and dioxaporphyrins may be considered to lie between two ligand categories, namely regular porphyrins and mono- and diheteroporphyrins of S, Se, and Te. We have previously stated that five-coordinate complexes of monoheteroporphyrin are geometrically and magnetically similar to their *N*-methylporphyrin counterparts.[13, 48] 21-Oxaporphyrin and 21,23-dioxaporphyrin act as the monoanionic or neutral ligand as expected for heteroporphyrins. Electronegativity causes the oxygen σ-donor properties to drop below even nitrogen, which is more electronegative than sulfur or selenium. The size of the coordinating centers N_3O or N_2O_2 discussed above matches the geometry of regular porphyrins.

The structure of $[(O_2TPPH)_2][NiCl_4]$, which is composed of two separate ionic units, the O_2TPPH^+ cation and the $[NiCl_4]^{2-}$ anion, may serve as a suitable structural model for the other diheteroporphyrins where the insertion of the metal ion was previously attempted.[23]

Experimental Section

Solvents and reagents: [D]Chloroform (Glaser) and [D_8]toluene (CIL) were used as received. All common solvents were purified by standard methods and distilled prior to use. 2,5-Bis(hydroxymethyl)furan, pyridinium dichromate, diethyl ether, and [D_5]pyrrole were supplied by Aldrich.

Furan-2,5-dicarboxaldehyde: 2,5-Bis(hydroxymethyl)furan (3.5 g, 27 mmol) was oxidized with a slurry of pyridinium dichromate (30 g) in dichloromethane (400 mL) for 24 h. When oxidation was completed the solid matter was filtered off, the solution volume was reduced to 100 mL, and 100 mL of diethyl ether was added. The resulting precipitate was filtered. The solution was evaporated under vacuum; during evaporation a white precipitate formed, which was collected by filtration, washed with ether, and dried in vacuo to yield 2 g of furan-2,5-dicarboxaldehyde (yield 60%). ^1H NMR (300 MHz, $CDCl_3$, 293 K): $\delta = 9.84$ (s, 2H), 7.31 (s, 2H).

2,5-Bis(phenylhydroxymethyl)furan: This compound was synthesized in a one-pot preparation by addition of phenylmagnesium bromide (20 mL, 1 M solution) in diethyl ether to an ether solution (300 mL) containing furan-2,5-dicarboxaldehyde (1 g, 8 mmol). After 30 min, 1% sulfuric acid (20 mL) was added. Subsequently solid Na_2CO_3 was added until the liberation of CO_2 ceased. The organic phase was separated from the $MgCO_3$ precipitate by filtration, and from the water layer. Then the organic phase was dried with $MgSO_4$ and concentrated under reduced pressure to afford crude 2,5-bis(phenylhydroxymethyl)furan as a pale yellow oil. ^1H NMR (300 MHz, $CDCl_3$, 293 K): $\delta = 7.41$ (m, 10H), 6.03 (s, 2H), 5.78 (d, 2H), 4.85 (b, 2H). The compound is sufficiently pure (>95% by ^1H NMR) for use in subsequent reactions.

5,20-Bis(*p*-tolyl)-10,15-diphenyl-21-oxaporphyrin (ODTDPPH): This compound was synthesised as previously described [12] from 2,5-bis(*p*-tolylhydroxymethyl)furan as the precursor. Oxaporphyrin deuterated in the β-pyrrole positions ([D_6]ODTDPPH) was obtained in the same way from [D_5]pyrrole.

5-Phenyl-10,15-bis(*p*-tolyl)-21-oxaporphyrin (OPDTPH): 2,5-Bis(hydroxymethyl)furan (7 g, 55 mmol) was oxidized with a slurry of pyridinium dichromate (16 g) in dichloromethane (800 mL) for 12 h. The reaction progress was checked by ^1H NMR. Under these conditions the product mixture contained ≈50% of the desired 2-carboxaldehyde-5-hydroxymethylfuran accompanied by the furan-2,5-dicarboxaldehyde. When oxidation was completed the volume was reduced to 150 mL and diethyl ether (200 mL) was added. The resulting precipitate was removed by filtration. The solvent was evaporated and a mixture of aldehydes (1.9 g) was dissolved in diethyl ether (300 mL). The Grignard reagent (phenylmagnesium bromide) was added as 1 M solution in diethyl ether (30 mL). The products were concentrated under reduced pressure to produce a pale yellow oil that contained a mixture of 2-(phenylhydroxymethyl)-5-(hydroxymethyl)furan and 2,5-(phenylhydroxymethyl)-furan. This mixture was used without further purification for the next step. The oil was dissolved in deoxygenated dichloromethane (500 mL), and benzaldehyde (2.15 mL, 18 mmol) and pyrrole (1.4 mL, 21 mmol) were added. After addition of boron trifluoride etherate (4 mmol) the reaction mixture was stirred for 1 h in the dark. *p*-Chloranil (5.9 g, 24 mmol) was added and the solution was refluxed (1 h) and then taken to dryness under reduced pressure by rotary evaporation. The product was dissolved in dichloromethane and chromatographed on a neutral alumina column to remove tarry products, followed by chromatography on basic alumina. Two fractions containing 5,20-diphenyl-10,15-bis(*p*-tolyl)-21-oxaporphyrin (ODPDTPH) and OPDTPH were eluted with chloroform, evaporated to dryness, and recrystallized from methanol/dichloromethane (1:1 v/v) to produce ODPDTPH (55 mg) and OPDTPH (40 mg). Anal. calcd for $OPDTPH \cdot 0.5\,CH_2Cl_2$ ($C_{40}H_{29}N_3O \cdot 0.5\,CH_2Cl_2$): C 79.65, H 4.92, N 6.88; found: C 80.08, H 4.83, N 6.79; ^1H NMR (300 MHz, $CDCl_3$, 213 K): $\delta = 10.24$ (s), 9.78 (d), 9.40 (d, $^3J = 4.7$ Hz), 9.17 (d), 8.88 (d, $^3J = 4.6$ Hz), 8.94 (m, 2H), 8.68 (d), 8.59 (d, $^3J = 4.9$ Hz), 8.20 (m, 2H), 8.08 (m, 4H), 7.79 (m, 3H), 7.56 (m, 4H), 2.69 (s, 3H), 2.67 (s, 3H), −2.06 (s, 1H); UV/Vis: λ [nm] (log ε) = 418 (4.97), 534 (sh), 504 (3.68), 474 (sh), 606 (3.01), 664 (2.78).

O_2TPP: 2,5-Bis(phenylhydroxymethyl)furan (1 g, 3 mmol) and pyrrole (0.2 mL, 3 mmol) were added to deoxygenated dichloromethane (500 mL). After addition of boron trifluoride etherate (0.5 mmol) the reaction mixture was stirred for 1 h in the dark. *p*-Chloranil (0.75 g, 3 mmol) was added and the solution was heated under reflux (1 h) and then taken to dryness under reduced pressure by rotary evaporation. The product was dissolved in dichloromethane and chromatographed on a neutral alumina column to remove tarry products, followed by chromatography on basic alumina. The O_2TPP fraction (orange-brown band) was eluted with dichloromethane, evaporated to dryness, and recrystallized from dichloromethane/ethanol (1:1 v/v) to produce 90 mg of dioxaporphyrin (yield 10%). Dioxaporphyrin deuterated in the β-pyrrole positions ([D_4]O_2TPP) was obtained in the same way from [D_5]pyrrole. Anal. calcd for $O_2TPP \cdot EtOH$ ($C_{44}H_{28}N_2O_2 \cdot C_2H_5OH$): C 83.36, H 5.17, N 4.23; found: C 83.42, H 4.70, N 4.38; ^1H NMR (300 MHz, $CDCl_3$, 295 K): $\delta = 9.08$ (s, 4H), 9.37 (s, 4H), 8.137 (m, 8H), 7.73 (m, 12H); UV/Vis: λ [nm] (log ε) = 416 (4.99), 466 (sh), 496 (4.19), 526 (3.67), 640 (3.25), 704 (3.54).

[(ODTDPP)Ni^{II}Cl]: A solution of nickel chloride tetrahydrate (200 mg, 1 mmol) in ethanol (5 mL) was added to a solution of 5,20-bis(*p*-tolyl)-10,15-diphenyl-21-oxaporphyrin (50 mg, 0.07 mmol) in chloroform (40 mL). The solution was heated under reflux for 2 h. It was cooled, and the solvent was removed under reduced pressure. The solid residue was extracted with chloroform, and the chloroform solution was separated from the remaining solid by filtration. The solution was subjected to column chromatography on silica gel (Mesh 70). Elution with chloroform gave a red fraction that was recovered as a solid after evaporation under vacuum. Recrystallization from dichloromethane/hexane (50/50) produced 59 mg of [(ODTDPP)Ni^{II}Cl] (yield 80%). Anal. calcd for (ODTDP)NiCl·CH_2Cl_2 ($C_{47}H_{34}N_3O \cdot CH_2Cl_2$): C 65.85, H 4.00, N 4.90; found: C 66.10, H 4.07, N 4.95; UV/Vis: λ [nm] (log ε) = 422 (4.54), 540 (3.32), 582 (3.31), 630 (2.55).

[(OPDTP)Ni^{II}Cl] was obtained in the same way from 5-phenyl-10,15-bis-(*p*-tolyl)-21-oxaporphyrin. UV/Vis: λ [nm] (log ε) = 421 (4.45), 430 (sh), 538 (3.35), 576 (3.37), 627 (2.53).

[(O_2TPP)$Ni^{II}Cl_2$]: A solution of $NiCl_2 \cdot 4H_2O$ (200 mg, 1 mmol) in methanol- (5 mL) was added to a solution of 5,10,15,20-tetraphenyl-21,23-dioxaporphyrin (50 mg, 0.08 mmol) in chloroform (40 mL). The solution was heated under reflux for 8 h. It was cooled, and the solvent was removed under

Table 3. Crystallographic data for [(ODTDPP)Ni^{II}Cl], [(ODTDPP)Ni^{I}], [(O$_2$TPP)Ni^{II}Cl$_2$], and [(O$_2$TPPH)$_2$][Ni^{II}Cl$_4$].

	[(ODTDPP)Ni^{II}]	[(ODTDPP)Ni^{I}]	[(O$_2$TPP)Ni^{II}Cl$_2$]	[(O$_2$TPPH)Ni^{II}Cl$_4$]
empirical formula	$C_{47}H_{34}Cl_3N_3NiO$	$C_{49}H_{35}N_3NiO$	$C_{46}H_{32}Cl_6N_2NiO_2$	$C_{46.5}H_{34}Cl_7N_2Ni_{0.5}O_2$
color, habit	black, hexagonal	black, parallelepiped	black, wedge	dark, needle
M_r	821.83	740.51	916.15	930.26
crystal system	monoclinic	triclinic	monoclinic	triclinic
space group	$P2_1/n$	$P\bar{1}$	$P2_1/n$	$P\bar{1}$
a (Å)	15.2750(10)	9.785(2)	10.8544(9)	12.7932(14)
b (Å)	11.1490(10)	13.104(3)	15.227(2)	13.3412(10)
c (Å)	22.705(2)	14.918(3)	25.398(2)	13.7131(11)
α (°)	90	103.82(3)	90	107.896(6)
β (°)	101.030(10)	106.54(3)	96.011(6)	104.236(7)
γ (°)	90	93.00(3)	90	96.116(7)
V (Å^3)	3795.3(5)	1765.6(6)	4174.7(7)	2116.7(3)
T (K)	130	130	130	130
Z	4	2	4	2
crystal size (mm)	0.33 × 0.28 × 0.15	0.12 × 0.10 × 0.08	0.22 × 0.12 × 0.12	0.26 × 0.08 × 0.08
ρ_{calcd} (g cm^{-3})	1.438	1.393	1.458	1.46
radiation λ (Å)	1.54178	1.54178	1.54178	1.54178
μ (Cu$_{K\alpha}$) (mm^{-1})	3.009	1.134	4.533	4.84
range of transm factors	0.45–0.68	0.87–0.92	0.39–0.63	0.63–0.73
R_1 [a,c]	0.1073	0.0846	0.0915	0.1213
$wR2$[b,c]	0.2266	0.1442	0.2105	0.3291
R_1 [d]	0.0806	0.0566	0.0735	0.0916

[a] $R_1 = \sum||F_o - F_c||/\sum|F_o|$. [b] $wR2 = [\sum[w(F_o^2 - F_c^2)^2]/\sum[w(F_o^2)^2]]^{1/2}$. [c] All data. [d] Data with $F_o > 2\sigma(F_o)$.

reduced pressure. The solid residue was extracted with chloroform, and the chloroform solution was separated from the remaining solid by filtration. Recrystallization from a dichloromethane/hexane mixture (70/30 v/v) and extended vacuum drying produced 50 mg of [(O$_2$TPP)Ni^{II}Cl$_2$] (yield 83%). Anal. calcd for $C_{44}H_{28}N_2O_2NiCl_2$: C 70.96, H 3.79, N 3.76; found: C 70.55, H 3.87, N 3.76; UV/Vis λ [nm] (log ε) = 406 (4.69), 494 (4.00), 524 (sh), 612 (3.08), 676 (3.36).

[(ODTDPP)Ni^{I}]: [(ODTDPP)Ni^{II}Cl] (20 mg) was dissolved in benzene and energetically stirred with zinc amalgam (2 h). The reducing agent was filtered off and the solution of [(ODTDPP)Ni^{I}] was taken to dryness under reduced pressure. All experiments were performed under nitrogen in a dry box (yield 10 mg). UV/Vis: λ [nm] = 370, 417, 515, 547.

(O$_2$TPP)$_2$[NiCl$_4$]: The acidic demetallation of [(O$_2$TPP)Ni^{II}Cl$_2$] (5 mg) was carried out in a dichloromethane/hydrochloric acid mixture. The dichloromethane layer was separated and evaporated to dryness. The product was recrystallized from dichloromethane/hexane to yield [(O$_2$TPPH)$_2$]-[Ni^{II}Cl$_4$]. The same product was obtained when O$_2$TPP (5 mg) in dichloromethane and NiCl$_2$ (20 mg) in concentrated hydrochloric acid (10 mL) were mixed together and the dichloromethane layer was separated, passed through a short, neutral alumina column, and evaporated to dryness. The product was recrystallized from dichloromethane/hexane (yield 3 mg). UV/Vis λ [nm] = 418, 519, 601, 664.

Instrumentation: ^{1}H NMR spectra were measured on a Bruker AMX spectrometer that operated in a quadrature detection mode. The signal-to-noise ratio was improved by apodization of the free induction decay, which typically induced 5–15 Hz broadening. The residual ^{1}H NMR spectra of the deuterated solvents were used as a secondary reference. The 2D COSY spectrum of [(ODTDPP)Ni^{II}Cl] was obtained after a standard 1D reference spectrum had been obtained. The 2D spectrum was recorded with 1024 points in t_2 over the desired bandwith (to include all desired peaks) with 256 t_1 blocks and 1024 scans per block. All experiments included four dummy scans prior to the collection of the first block.

EPR spectra were recorded on a Bruker ESP 300E spectrometer equipped with a Hewlett–Packard 5350B frequency counter. The magnetic field was calibrated by means of EPR standards.

X-ray structure determination:

Crystal preparation: Crystals of [(ODTDPP)Ni^{II}Cl]·CH$_2$Cl$_2$, [(O$_2$TPP)-Ni^{II}Cl$_2$], and [(O$_2$TPPH)$_2$][Ni^{II}Cl$_4$]·5CH$_2$Cl$_2$ were grown by diffusion of *n*-hexane into a dichloromethane solution of the appropriate complex in a thin tube. Crystals of [(ODTDPP)Ni^{I}]C$_6$H$_6$ were prepared by diffusion of acetonitrile into a benzene solution in a thin tube under strictly anaerobic conditions. Suitable crystals were coated with light hydrocarbon oil and mounted directly in the 130 K dinitrogen stream of the low-temperature apparatus.

X-ray data collection: Data were collected at 130 K on a Siemens P4/RA diffractometer equipped with a Siemens LT-2 low-temperature apparatus. Two check reflections showed random (less than 2%) variation during the data collection. The data were corrected for Lorentz and polarization effects. The radiation employed was Ni-filtered Cu$_{K\alpha}$ from a Siemens rotating anode source operating at 9 kW in the case of [(ODTDPP)Ni^{I}]·C$_6$H$_6$ and [(O$_2$TPPH)$_2$][Ni^{II}Cl$_4$]·5CH$_2$Cl$_2$; the normal focused sealed tube (monochromator graphite-filtered Cu$_{K\alpha}$) was used in the data collections for [(ODTDPP)Ni^{II}Cl]·CH$_2$Cl$_2$ and [(O$_2$TPP)Ni^{II}Cl$_2$]. Crystal data are compiled in Table 3.

Solution and structure refinement: Calculations were performed on a PC with SHELXTL v.5. Scattering factors for neutral atoms and corrections for anomalous dispersion were taken from the standard source [52]. An absorption correction was applied to the structures [53]. The solutions were obtained by direct methods.

[(ODTDPP)Ni^{II}Cl]·CH$_2$Cl$_2$: There is disorder in the oxygen atom location, and the N(3) atom was refined as coincident with O(1). The relative occupancies are 80.2% and 19.8%. A molecule of dichloromethane in the lattice exhibits six disordered positions for the chlorine atoms and three for the carbon atoms.

[(ODTDPP)Ni^{I}]·C$_6$H$_6$: The position of the oxygen atom is disordered over two positions in the proportions 56.9% and 43.1%. The disorder was treated by examining several different models that place the oxygen in the nitrogen site of the pyrrole group involving N(3). The occupancies were determined by requiring that two oxygen atoms have reasonable thermal parameters. Once determined from the latter difference maps the positions of O(1) and N(3), O(1)′ and N(3)′ were fixed during the refinement. A molecule of benzene in the lattice occupies two disordered positions with relative occupancies of 50%.

[(O$_2$TPP)Ni^{II}Cl$_2$]·2CH$_2$Cl$_2$: There is no apparent disorder in the position of the N and O atoms. One molecule of dichloromethane in the lattice is in an ordered position with one of the hydrogens interacting with the axial chloride ligand; the second dichloromethane has three disordered positions for the chlorine atoms.

[(O$_2$TPPH)$_2$Ni^{II}Cl$_4$]·5CH$_2$Cl$_2$: The structure was solved by direct methods. There is no apparent disorder in the positions of the N and O atoms. If their positions are switched the $R1$ value increases from 0.0941 to 0.0946 and the thermal parameters are skewed. The positive charge of the porphyrin cation is balanced by one half unit of NiCl$_4^{2-}$ in the asymmetric unit. The site is shared by one half of a molecule of CH$_2$Cl$_2$. Four other molecules of CH$_2$Cl$_2$ are also at one-half occupancy; carbon atoms were located for three of these. The fourth has two different sites for one of the chlorine atoms: Cl(11), 0.5 occupancy; Cl(12) and Cl(13), 0.25 occupancy. Distance restraints of C–Cl 1.77(1) Å and Cl···Cl 2.89(2) Å were applied to the atoms of the

disordered CH_2Cl_2's. There is rotational disorder that involves one of the phenyl rings, C(33) to C(38). This was modeled by the use of two equal sets of carbon atoms, set A and set B (refined as a rigid group). Hydrogen atoms were included at their geometrically idealized positions and refined by use of a riding model. The hydrogen bonded to N(2) was located in a difference Fourier map before being thus positioned. All hydrogen thermal parameters were 20% greater than the equivalent isotropic thermal parameter of the bonded atom. Refinement was by full-matrix least-squares methods, based on F^2, from all data with anisotropic thermal parameters for non-hydrogen atoms except for the carbons of the disordered phenyl group. The largest peaks in the final difference map were less than 0.74 $e\,Å^{-3}$.

Crystallographic data (excluding structure factors) for the structures reported in this paper have been deposited with the Cambridge Crystallographic Data Centre as supplementary publication no. CCDC-1220-47. Copies of the data can be obtained free of charge on application to the Director, CCDC, 12 Union Road, Cambridge CB21EZ, UK (Fax: int. code +(1223)336-033; e-mail: teched@chemcrys.cam.ac.uk).

Acknowledgments: Financial support from the State Committee for Scientific Research KBN of Poland (Grant 3T09A14309) and US National Science Foundation (US–Poland Cooperative Science Program Grant INT-9114389) is gratefully acknowledged.

Received: August 13, 1996 [F442]

---

[1] M. J. Broadhurst, R. Grigg, A. W. Johnson, *J. Chem. Soc. C* **1971**, 3681.

[2] a) T. J. King, J. C. McGorley, Nottingham University, unpublished results; b) J. C. McGorley, Ph.D. Thesis, Nottingham University, **1967**.

[3] a) T. D. Lash, Y. G. Motta, *Heterocycles* **1983**, 20, 2343; b) T. D. Lash, Y. L. S.-T. Armiger, *J. Heterocycl. Chem.* **1991**, *28*, 965; c) T. D. Lash, *J. Org. Chem.* **1992**, *57*, 4312.

[4] a) E. Vogel, W. Haas, B. Knipp, J. Lex, H. Schmickler, *Angew. Chem. Int. Ed. Engl.* **1988**, *27*, 406, *Angew. Chem.* **1988**, *100*, 445; b) E. Vogel, J. Dörr, A. Herrmann, J. Lex, H. Schmickler, P. Walgenbach, J. P. Gisselbrecht, M. Gross, *ibid.* **1993**, *32*, 1600, and **1993**, *105*, 1667; c) E. Vogel, M. Sicken, P. Röhrig, H. Schmickler, J. Lex, O. Ermer, *ibid.* **1988**, *27*, 411, and **1988**, *100*, 450.

[5] a) G. Märkl, H. Sauer, P. Kreitmeier, T. Burgermeister, F. Kastner, G. Adolin, H. Nöth, K. Polborn, *Angew. Chem. Int. Ed. Engl.* **1994**, *33*, 1151, *Angew. Chem.* **1994**, *106*, 1211; b) E. Vogel, *Pure Appl. Chem.* **1993**, *63*, 143.

[6] J. L. Sessler, A. K. Burrell, *Top. Curr. Chem.* **1992**, *161*, 179, and references cited therein.

[7] M. J. Broadhurst, R. Grigg, A. W. Johnson, *J. Chem. Soc. Perkin I* **1972**, 2111.

[8] D. C. Miller, M. R. Johnson, J. J. Becker, J. A. Ibers, *J. Heterocycl. Chem.* **1993**, *30*, 1485.

[9] D. C. Miller, M. R. Johnson, J. A. Ibers, *J. Org. Chem.* **1994**, *59*, 2877.

[10] a) M. J. Broadhurst, R. Grigg, A. W. Johnson, *J. Chem. Soc. Perkin I* **1972**, 1124; b) P.-Y. Heo, K. Shin, C.-H. Lee, *Tetrahedron Lett.* **1996**, *37*, 197.

[11] A. L. Balch, L. Latos-Grażyński, B. C. Noll, M. M. Olmstead, L. Szterenberg, N. Safari, *J. Am. Chem. Soc.* **1993**, *115*, 1422, and references cited therein.

[12] L. Latos-Grażyński, E. Pacholska, P. J. Chmielewski, M. M. Olmstead, A. L. Balch, *Angew. Chem. Int. Ed. Engl.* **1995**, ***34***, 2252; *Angew. Chem.* **1995**, *107*, 2647.

[13] a) L. Latos-Grażyński, J. Lisowski, M. M. Olmstead, A. L. Balch, *Inorg. Chem.* **1989**, *28*, 1183; b) J. Lisowski, L. Latos-Grażyński, L. Szterenberg, *Inorg. Chem.* **1992**, *31*, 1933; c) P. J. Chmielewski, L. Latos-Grażyński, *ibid.* **1992**, *31*, 5231.

[14] a) R. P. Pandian, T. K. Chandrashekar, *J. Chem. Soc. Dalton Trans.* **1993**, 119; b) R. P. Pandian, T. K. Chandrashekar, *Inorg. Chem.* **1994**, *33*, 3317.

[15] a) P. J. Chmielewski, M. Grzeszczuk, L. Latos-Grażyński, J. Lisowski, *Inorg. Chem.* **1989**, ***28***, 3546; b) L. Latos-Grażyński, M. M. Olmstead, A. L. Balch, *Inorg. Chem.* **1989**, *28*, 4065. c) P. Chmielewski, L. Latos-Grażyński, E. Pacholska, *ibid.* **1994**, ***33***, 1992.

[16] L. Latos-Grażyński, E. Pacholska, P. J. Chmielewski, M. M. Olmstead, A. L. Balch, *Inorg. Chem.* **1996**, ***35***, 566.

[17] D. E. Fenton, D. H. Cook, I. W. Nowell, P. E. Walker, *J. Chem. Soc. Chem. Comm.* **1977**, 623.

[18] C. E. Kyriadikis, P. C. Christidis, P. J. Rentzeperis, I. A. Tossidis, C. A. Bolos, *Z. Kristallogr.* **1990**, *193*, 101.

[19] a) M. G. B. Drew, F. S. Esho, S. Nelson, *J. Chem. Soc. Dalton Trans.* **1983**, 1653; b) S. M. Nelson, F. S. Esho, M. G. B. Drew, *ibid.* **1983**, 1857; c) H. Adams, N. A. Bailey, D. E. Fenton, R. J. Good, R. Moody, C. O. Rodriguez de Barbarin, *ibid.* **1987**, 207.

[20] R. Crescenzi, E. Solari, C. Floriani, A. Chiesi-Villa, C. Rizzoli, *Inorg. Chem.* **1996**, *35*, 2413.

[21] M. Sabat, M. F. Gross, M. G. Finn, *Organometallics* **1992**, *11*, 745.

[22] a) M. Veith, C. Ruloff, V. Huch, F. Töllner, *Angew. Chem. Int. Ed. Engl.* **1988**, *27*, 1381; *Angew. Chem.* **1988**, *100*, 1418; b) K. H. Pannel, R. Cea-Olivares, R. A. Toscano, R. N. Kapoor, *Organometallics* **1987**, *6*, 1821; c) H. E. Selnau, J. S. Merola, *ibid.* **1993**, *12*, 1253; d) H. E. Selnau, J. S. Merola, *ibid.* **1993**, *12*, 3800; e) W. D. Jones, L. Dong, A. W. Myers, *ibid.* **1995**, *14*, 855; f) H.-G. Shu, L.-H. Shiu, S.-H. Wang, S.-L. Wang, G.-H. Lee, S.-M. Peng, R.-S. Liu, *J. Am. Chem. Soc.* **1996**, *118*, 530.

[23] a) A. Ulman, J. Manassen, *J. Am. Chem. Soc.* **1975**, *97*, 6540; b) A. Ulman, J. Manassen, F. Frolow, D. Rabinowich, *Tetrahedron Lett.* **1978**, 167; c) A. Ulman, J. Manassen, F. Frolow, D. Rabinowich, *ibid.* **1978**, 1885.

[23] A. Ulman, J. Manassen, *J. Chem. Soc. Perkin Trans. 1* **1979**, 1066.

[24] J. Lisowski, M. Grzeszczuk, L. Latos-Grażyński, *Inorg. Chim. Acta.* **1989**, *161*, 153.

[25] a) G. N. La Mar, F. A. Walker in *Porphyrins* (Ed.: D. Dolphin), Academic Press, New York, **1979**, Vol. IVB, p. 61; b) I. Bertini, C. Luchinat, *NMR of Paramagnetic Molecules in Biological Systems,* Benjamin/Cumming, Menlo Park, CA, **1986**.

[26] K. A. Keating, J. S. de Ropp, G. N. La Mar, A. L. Balch, F.-Y. Shiau, K. M. Smith, *Inorg. Chem.* **1991**, *30*, 3258.

[27] F. A. Walker, U. Simonis in *Biological Magnetic Resonance, Volume 12: NMR of Paramagnetic Molecules* (Eds.: L. J. Berliner, J. Reuben), Plenum, New York, **1993**, p. 133.

[28] K. Rachlewicz, L. Latos-Grażyński, *Inorg. Chem.* **1996**, *35*, 1136.

[29] J. P. Jesson in *NMR of Paramagnetic Molecules* (Eds.: G. N. La Mar, W. D. Horrocks, Jr., R. H. Holm), Academic Press, New York, **1974**, pp. 2–51; W. D. Horrocks, Jr., *ibid.*, pp. 128–175.

[30] a) R. J. Kurland, B. R. McGarvey, *J. Magn. Reson.* **1970**, *2*, 286; b) B. J. Bleaney, *ibid.* **1972**, *8*, 91.

[31] a) L. Latos-Grażyński, *Inorg. Chem.* **1985**, *24*, 1681; b) P. J. Chmielewski, L. Latos-Grażyński, T. Głowiak, *J. Am. Chem. Soc.* **1996**, *118*, 5690.

[32] The half-wave potential for the reversible ($\Delta V = 66$ mV) reduction process of [(ODTDPP)Ni^{II}Cl] is $E_{1/2} = -0.62$ V vs. SCE in acetonitrile with 0.1 M TBA as the supporting electrolyte.

[33] J. F. Kirner, J. Garofolo, Jr., W. R. Scheidt, *Inorg. Nucl. Chem. Lett.* **1975**, *11*, 107.

[34] C. Kratky, A. Fässler, A. Pfaltz, B. Kräutler, B. Jaun, A. Eschenmoser, *J. Chem. Soc. Chem. Commun.* **1984**, 1368.

[35] H. J. Goodwin, K. Henrick, L. F. Lindoy, M. McPartlin, P. A. Tasker, *Inorg. Chem.* **1982**, *21*, 3261.

[36] B. Bosnich, M. Mason, P. J. Pauling, G. B. Robertson, M. L. Tobe, *J. Chem. Soc. Chem. Commun.* **1965**, 97.

[37] A. Małek, L. Latos-Grażyński, T. Bartczak, A. Żądło, *Inorg. Chem.* **1991**, *30*, 3223.

[38] a) L. R. Furelind, M. W. Renner, K. M. Smith, J. Fajer, *J. Am. Chem. Soc.* **1990**, *112*, 1634; b) L. R. Furelind, M. W. Renner, J. Fajer, *ibid.* **1990**, *112*, 8987; c) M. W. Renner, L. R. Furelind, K. M. Barkigia, A. Forman, H.-K. Shim, D. J. Simpson, K. M. Smith, J. Fajer, *ibid.* **1991**, *113*, 6891; d) L. R. Furelind, M. W. Renner, D. J. Szalada, E. Fujita, *ibid.* **1991**, *113*, 883; e) M. P. Suh, H. K. Kim, M. J. Kim, K. Y. Oh, *Inorg. Chem.* **1992**, *31*, 3620.

[39] a) A. Gleizes, M. Y. Dartiguenave, J. Galy, H. F. Klein, *J. Am. Chem. Soc.* **1977**, *99*, 5187; b) M. M. Olmstead, W. K. Musker, R. M. Kessler, *Inorg. Chem.* **1981**, *20*, 151; c) W. K. Musker, M. M. Olmstead, R. M. Kessler, *ibid.* **1984**, *23*, 3266.

[40] a) T. Mashiko, C. A. Reed, K. J. Haller, W. R. Scheidt, *Inorg. Chem.* **1984**, *23*, 2958; b) P. Doppelt, J. Fischer, R. Weiss, *ibid.* **1984**, *23*, 2958.

[41] a) M. J. Hamor, T. A. Hamor, J. L. Hoard, *J. Am. Chem. Soc.* **1964**, *86*, 1938; b) S. J. Silvers, A. Tulinsky, *ibid.* **1967**, *89*, 3331.

[42] a) P. Pauling, *Inorg. Chem.* **1966**, *5*, 1498; b) G. D. Stucky, J. B. Folkers, T. J. Kistenmacher, *Acta Crystallogr.* **1967**, *23*, 1064; c) P. B. Hitchcock, K. R. Seddon, T. Welton, *J. Chem. Soc. Dalton Trans.* **1993**, 2639.

[43] R. Fourme, *Acta Crystallogr. Sect. B.* **1972**, *28*, 2984.

[44] L. Latos-Grażyński, J. Lisowski, L. Szterenberg, M. M. Olmstead, A. L. Balch, *J. Org. Chem.* **1991**, *5*, 4043.

[45] a) P. J. Chmielewski, L. Latos-Grażyński, K. Rachlewicz, T. Głowiak, *Angew. Chem. Int. Ed. Engl.* **1994**, *33*, 779; *Angew. Chem.* **1994**, *106*, 805; b) P. J. Chmielewski, L. Latos-Grażynski, *J. Chem. Soc. Perkin Trans. 2* **1995**, 503.

[46] H. Furuta, T. Asano, T. Ogawa, *J. Am. Chem. Soc.* **1994**, *116*, 767.

[47] a) A. M. Stolzenberg, A. M. Sterschic, *Inorg. Chem.* **1987**, *26*, 3082; b) A. M. Stolzenberg, A. M. Sterschic, *J. Am. Chem. Soc.* **1988**, *110*, 5397; c) A. M. Stolzenberg, A. M. Sterschic, *ibid.* **1988**, *110*, 6391; d) W. R. Scheidt, Y. Lee, *J. Struct. Bonding* **1987**, *64*, 61.

[48] D. K. Lavallee, *The Chemistry and Biochemistry of N-Substituted Porphyrins*, VCH, New York, **1987**.

[49] M. A. Halcrow, G. Christou, *Chem. Rev.* **1994**, *94*, 2421.

[50] a) A. Pfaltz in *The Bioinorganic Chemistry of Nickel* (Ed.: J. R. Lancaster, Jr.,) VCH, New York, **1988**, p. 275; b) B. Jaun in *Metal Ions in Biological Systems* (Eds.: H. Sigel, A. Sigel), Marcel Dekker, New York, **1993**, Vol. 29, p. 287.

[51] S. P. J. Albracht, D. Ankel-Fusch, R. Boccher, J. Ellerman, J. Mol, J. W. Van der Zwaan, J. K. Thauer, *Biochim. Biophys. Acta.* **1988**, *955*, 86.

[52] *International Tables for X-ray Crystallography*, D. Reidl, Boston, **1991**, Vol. C.

[53] The program XABS2 calculates 24 coefficients from a least-squares fit of A^{-1} and $\sin^2(\theta)$ to a cubic equation in $\sin^2(\theta)$ by minimization of F_o^2 and F_c^2 differences. S. Parkin, B. Moezzi, H. Hope, *J. Appl. Cryst.* **1995**, *28*, 53.